

FIG. 6. Possible level structure at the two sites deduced from our simple model and experimental results. $\Delta_1 \approx 250^\circ\text{K}$; $\Delta_2 \approx 850^\circ\text{K}$.

orbital levels at both sites. Using Eqs. (3) and (6) to fit the shape of the curves in Fig. 3 gives the approximate energy-level splittings (Δ_1, Δ_2) at the two sites. Figure 6 shows the level structure for our idealized model in which we find $\Delta_1 \approx 250^\circ\text{K}$ and $\Delta_2 \approx 850^\circ\text{K}$.

V. CONCLUSIONS

It is clear that one-half of the ferrous ions in ferrous formate are located at sites where the effective electric-field gradient is appreciably different from that at the

location of the other half. The smaller electric-field gradient occurs at the site possessing approximately octahedral symmetry (type-1 sites). Further evidence for this assignment is found when the absorber is taken to a lower temperature.⁸

Our experimental results (Fig. 3) show that the quadrupole coupling constant increases more rapidly with decreasing temperature at the type-1 sites indicating that the ion orbital levels are closer together at that site. According to our calculations the magnitudes of the electric-field gradients at the two sites at low temperatures are consistent with the assignment of the ground orbital state at the type-1 sites as a doublet and at the type-2 sites a singlet.

ACKNOWLEDGMENTS

It is a great pleasure for us to acknowledge the inspiration and counsel of Professor S. DeBenedetti. We had many stimulating discussions with Professor S. A. Friedberg, Mrs. S. de S. Barros, and Dr. George Wagner. We also thank Dr. J. Skalyo for advice on low-temperature measurements and Dr. R. Ingalls for a helpful communication.

Band Structure of Silver Chloride and Silver Bromide*

PETER M. SCOP†

Massachusetts Institute of Technology, Cambridge, Massachusetts

(Received 12 January 1965; revised manuscript received 26 March 1965)

The valence and conduction bands of silver chloride and silver bromide were calculated using the augmented-plane-wave (APW) method. For both crystals the calculated bands were adjusted so that the experimental value of the direct band gap at Γ was duplicated ($E_g = 5.13$ eV in AgCl, $E_g = 4.29$ eV in AgBr). Several possible correction terms to the APW potential were considered. The effects of the nonspherical cubic field inside APW spheres and the varying cubic field outside the spheres were negligible. The mass-velocity correction was large for states which arise from the $\text{Ag}^+(4d)$ electron. The calculated indirect band gaps were 3.28 and 2.89 eV for AgCl and AgBr, respectively. These values are within 10% of the experimental values. The indirect gap may occur along the [110] direction or at the point L .

I. INTRODUCTION—APW CALCULATIONS

THE augmented-plane-wave (henceforth abbreviated APW) method has been employed in calculating the electronic band structure of silver chloride and silver bromide crystals. This method was originally proposed by Slater¹ and later used by Wood² in his calculation of the band structure of iron. More recently,

Switendick³ has extended the method to deal with problems involving two atoms per unit cell in his band calculation of nickel oxide. The APW calculation of the band structure of silver chloride and silver bromide has been performed using the programs written by Wood and Switendick for the IBM 709 computer.

In the APW method the one-electron potential energy is constructed as follows. Spheres are inscribed about each ionic site in the crystal; within each sphere the potential energy of an electron is assumed to be the

* Research supported by the U. S. Office of Naval Research and the National Science Foundation.

† Presently employed by the National Research Corporation, a Subsidiary of Norton Company, Cambridge, Massachusetts.

¹ J. C. Slater, *Phys. Rev.* **51**, 846 (1937).

² J. H. Wood, *Phys. Rev.* **126**, 517 (1962).

³ A. C. Switendick, MIT Solid-State and Molecular Theory Group, Quarterly Progress Report No. 49, July 1962 (unpublished).

spherical average of the one-electron potential energy for an electron in the appropriate ion. In the region between spheres, the potential is assumed to be constant and put equal to zero.

Corresponding to this choice of potential energy, the one-electron wave function is expanded in augmented plane waves. An APW is a plane wave outside the spheres, joined continuously to a solution of the spherical-potential problem corresponding to a definite energy inside the spheres. The assumed solution to the one-electron problem in the crystal is a linear combination of APW's, the coefficients being determined by a secular equation. The last step in the process is to equate the assumed energy inside the spheres to the eigenvalues of the secular equation.

Since the APW functions are constructed to correspond to the assumed potential, the convergence (the number of APW's needed to adequately represent a particular state) will be fairly rapid. However, one must face some serious questions about the validity of the assumed potential.

The general form of this potential is sensible from physical reasoning, but the problem of choosing the various parameters entering into the calculations is a difficult one. One must determine the sizes of the APW sphere radii; in addition, the ionic potentials themselves usually depend on several parameters, especially the "ionicity" (the limit of $r/2$ times the ionic potential, for large r).

If one attempts to choose these parameters by physical reasoning, the results may be quite confusing. For example, in a real ionic crystal the previous simple definition of ionicity cannot even be applied since an electron never experiences a single ionic potential far from ionic sites. In addition, the concept of sphere radii may be misleading if there is any covalent bonding in the crystal.

In order to avoid these (and other) physical arguments, the present author has chosen the parameters in a rather arbitrary manner, and then varied one of them in order to obtain some agreement with experimental results.

II. DETAILS OF THE CALCULATIONS FOR AgBr AND AgCl

AgBr and AgCl both have the NaCl structure, that is, two displaced face-centered cubic lattices. One lattice is composed of silver ions, the other contains the halogen ions. A silver ion is located at the origin of coordinates. The six neighboring halogen ions are located at the points $\pm\frac{1}{2}a(1,0,0)$, $\pm\frac{1}{2}a(0,1,0)$, $\pm\frac{1}{2}a(0,0,1)$. There are 12 nearest-neighbor silver ions located at $\pm\frac{1}{2}a(1,1,0)$, $\pm\frac{1}{2}a(1,-1,0)$, $\pm\frac{1}{2}a(0,1,1)$, $\pm\frac{1}{2}a(0,1,-1)$, $\pm\frac{1}{2}a(1,0,1)$, $\pm\frac{1}{2}a(1,0,-1)$. All translations which leave the lattice invariant are given by $\mathbf{T}(n_1, n_2, n_3) = n_1\mathbf{a}_1 + n_2\mathbf{a}_2 + n_3\mathbf{a}_3$ where n_1, n_2, n_3 are integers and $\mathbf{a}_1, \mathbf{a}_2, \mathbf{a}_3$ are three primitive translations:

$\mathbf{a}_1 = \frac{1}{2}a(0,1,1)$; $\mathbf{a}_2 = \frac{1}{2}a(1,0,1)$; $\mathbf{a}_3 = \frac{1}{2}a(1,1,0)$. For AgCl $\frac{1}{2}a = 5.23$ a. u., for AgBr, $\frac{1}{2}a = 5.46$ a. u.⁴ (a. u. = atomic units).

The ionicity parameters were chosen in accordance with the ordinary ideas of chemical valence (i. e., ionicity of $\text{Ag}^+ = +1$, ionicity of $\text{Cl}^- = \text{ionicity of Br}^- = -1$).

The free-ion one-electron potential energies used are those determined by the Hartree-Fock-Slater equations and calculated using programs described by Herman and Skillman.⁵

These potential energy functions for an electron within each sphere are modified in two ways. First the Madelung energy

$$V_M = -2\alpha/(a/2) = -4\alpha/a$$

($\alpha = 1.747558$ is the Madelung constant for an NaCl structure⁶) is added to or subtracted from the original potential energy. That is,

about silver sites $V(r) = (V_{\text{Herman-Skillman}})_{\text{Ag}^+} - V_M$;

about halogen sites $V(r) = (V_{\text{Herman-Skillman}})_{\text{halogen}} + V_M$.

Finally a positive constant V_0 is added to the potential energy in each sphere. This constant will be treated as an adjustable parameter that is eventually determined by fitting the calculated value of the band gap at $\mathbf{k} = 0$ to the experimental value.

The choice of the sphere radii and the initial determination of V_0 were made in the following way. First the Herman-Skillman free-ion potential energies for Ag^+ and Cl^- were superimposed and plotted in the [100] direction [Fig. 1(a)]. Then these potential energies were corrected by adding or subtracting the Madelung energy. The point where the Madelung-corrected potential energies cross defines the sphere radii and the first determination of V_0 [Fig. 1(b)]. The net result of the Madelung correction and addition of V_0 is that the Herman-Skillman potential energies have been altered by different amounts called V_{shift} :

$$\begin{aligned} \text{for Ag}^+ \quad V_{\text{shift}} &= V_0 - V_M, \\ \text{for halogen} \quad V_{\text{shift}} &= V_0 + V_M. \end{aligned}$$

Thus, the corrected potential energies become:

for Ag^+ $V(r) = (V_{\text{Herman-Skillman}})_{\text{Ag}^+} + (V_{\text{Ag}^+})_{\text{shift}}$;

for halogen

$$V(r) = (V_{\text{Herman-Skillman}})_{\text{halogen}} + (V_{\text{shift}})_{\text{halogen}}.$$

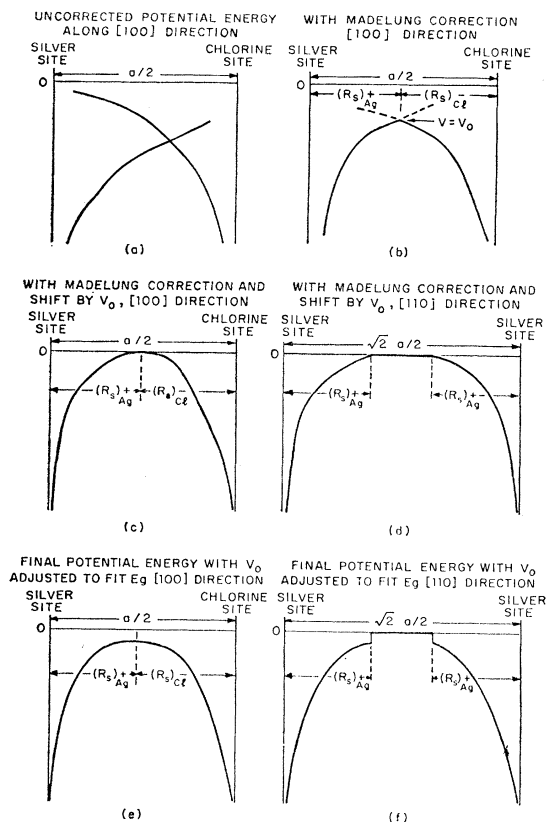
This corrected potential energy is shown in Figs. 1(c) and 1(d) for the [100] and [110] directions.

When the above scheme is used in determining the sphere radii and V_0 , the bands subsequently found do

⁴ R. Wyckoff, *Crystal Structures* (Interscience Publishers, Inc., New York, 1963), 2nd ed., Vol. I, p. 86.

⁵ F. Herman and S. Skillman, *Atomic Structure Calculations* (Prentice-Hall, Inc., Englewood Cliffs, New Jersey, 1963).

⁶ C. Kittel, *Introduction to Solid-State Physics* (John Wiley & Sons, Inc., New York, 1956), 2nd ed., p. 77.

FIG. 1. Determination of V_0 and sphere radii.

not agree with experimental facts. Specifically, the band gap at $k=0$ is too small for both AgCl and AgBr. This discrepancy may be resolved by varying the magnitude of V_0 until agreement with experiment is obtained. For both AgCl and AgBr the experimental band gap at $k=0$, E_g , was duplicated when the magnitude of V_0 was reduced. The final form of the potential energy is shown in Figs. 1(e) and 1(f) for the $[100]$ and $[110]$ directions, respectively.

This corrected potential energy should be more representative of the actual crystalline potential energy than that shown in Figs. 1(c) and 1(d). Along the line joining the APW sphere centers (x , y , or z directions) the ionic potential energies employed will have some value V at the sphere radii. However, in some other direction the actual crystalline potential energy just beyond either of the APW spheres will not be equal to V as in Fig. 1(d), but will have some larger value as in our corrected potential energy [Fig. 1(f)]. Hence, a jump discontinuity in the potential energy at the sphere radii is needed to allow the APW method to represent the behavior of the potential energy in different directions. The magnitude of this discontinuity is the difference of the initial value of V_0 [which makes $V(r)$ continuous] and the final value of V_0 needed to fit E_g . For AgCl this jump is $0.869357 - 0.579357 = 0.29$ Ry; for AgBr it is $0.87501 - 0.69465 = 0.18036$ Ry.

Although the size of the band gap at $k=0$ depends in a critical way on the value of V_0 , the relative spacing of core and valence states is almost independent of this quantity. This corresponds to the physical fact that the charge density associated with the p and d states lies almost entirely within the APW spheres. Hence, varying V_0 shifts the valence bands rigidly relative to the conduction band. In fact, changing V_0 by as much as a few tenths of a rydberg only altered the relative spacings of valence bands by less than 0.01 Ry and left their qualitative features virtually unchanged.

The APW bands for AgCl and AgBr are shown in Figs. 2 and 3, respectively. Values for the sphere radii, V_{shift} , V_M , the free-ion potential energies as functions of r , and the points in the Brillouin zone actually calculated for the bands in Figs. 2 and 3 are given in Ref. 7.

At this point it should be mentioned that because our basis functions are located on different sites in the unit cell, the symmetry properties of certain eigenstates of the Hamiltonian depend on which ion is located at the origin of coordinates. Switendick⁸ has shown that within the Brillouin zone it makes no difference which ion is at the origin; but on the surface of the Brillouin zone, the representation matrices for the ion located at $\mathbf{R}_n = \frac{1}{2}a(1,0,0)$ must be multiplied by the factor

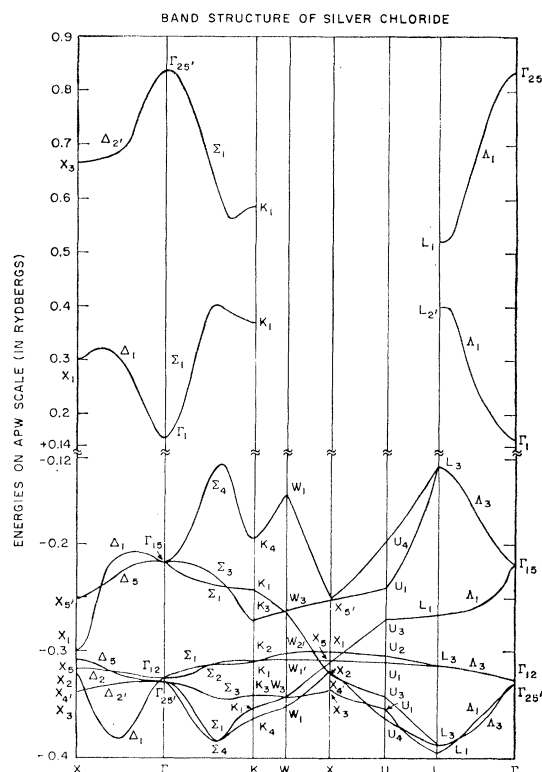


FIG. 2. Band structure of silver chloride.

⁷ P. M. Scop, MIT Solid-State and Molecular Theory Group, Quarterly Progress Report No. 54, October 1964 (unpublished).

⁸ A. C. Switendick, doctoral thesis, MIT (1963) (unpublished).

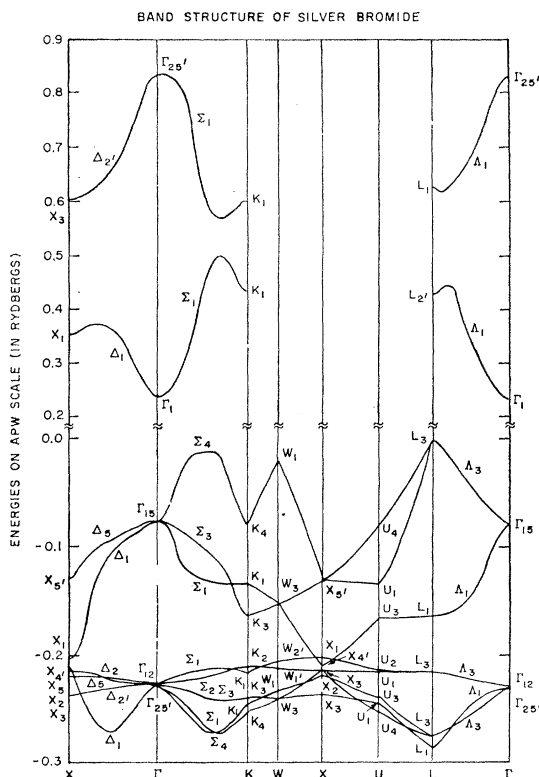


FIG. 3. Band structure of silver bromide.

$\exp[i(R\mathbf{K}_l - \mathbf{K}_l) \cdot \mathbf{R}_n]$ (here R is an operation of the group of the wave vector and \mathbf{K}_l is a vector of the reciprocal lattice). One finds that the symmetries at L , W , and Q are affected. The results are shown in Table I.

After solving the secular equations and obtaining eigenvalues, the eigenfunctions may also be determined. For points of major interest in the Brillouin zone, we have obtained the spherically-averaged radial charge densities within each APW sphere. The total amount of charge in each sphere associated with a given l value, q_l , and the amount of plane-wave charge (between spheres) have also been calculated and are tabulated in Ref. 7.

TABLE I. Representations for face-centered cubic structure displaying different symmetries about different centers.

Center A at origin	Center B at (a/2) (1,0,0)
L_1	$L_{2'}$
L_2	$L_{1'}$
L_3	$L_{3'}$
$L_{1'}$	L_2
$L_{2'}$	L_1
$L_{3'}$	L_3
W_1	$W_{3'}$
W_2	$W_{1'}$
$W_{1'}$	W_2
$W_{2'}$	W_1
W_3	W_3
Q_+	Q_-
Q_-	Q_+

In order to determine the slopes of the bands at symmetry points within and on the surface of the Brillouin zone, the expectation value of the momentum vector was determined using $\mathbf{k} \cdot \mathbf{p}$ perturbation theory and well known selection rules.⁹ Thus, because of parity, the slopes in any direction of all bands are zero at Γ , X and L . At U the bands have zero slope along U to W , but nonzero slope along U to X and U to L . At W the bands associated with the one-dimensional representations all have zero slope, the slopes of bands associated with representation W_3 are zero along W to L but nonzero along W to X , W to U , and W to K . At K the slopes of all bands are zero along K to W and nonzero along K to L and K to Γ .

III. DISCUSSION OF APW BANDS

The gross features of the APW bands shown in Figs. 2 and 3 are simply interpreted using the appropriate charge densities and symmetry of the various states. The lowest conduction band in either crystal arises mostly from s -like ionic functions and is nearly spherical in the neighborhood of its minimum at Γ_1 .

Most of the features of the wide valence band can be explained by the variation in strength of the interaction between states arising from the $\text{Cl}^- (3p)$ or $\text{Br}^- (4p)$ and $\text{Ag}^+ (4d)$ functions. Since the group of the wave vector at $\mathbf{k}=0$, (point group O_h) contains the inversion, the bands are parity eigenstates at Γ . By examining the charge within each APW sphere, the valence bands at this point are seen to arise predominantly from either p or d functions with no mixing of p and d states. At Γ_{15} the eigenfunction is mostly $\text{Cl}^- (3p)$ or $\text{Br}^- (4p)$ with some $\text{Ag}^+ (5p)$. The Γ_{12} and $\Gamma_{25'}$ states are almost entirely $\text{Ag}^+ (4d)$.

As one departs from along any of the three symmetry directions, the valence bands exhibit a strong p - d mixing.

In the $[100]$ or Δ direction, the p - d mixing is zero at Γ , increases until $\mathbf{k} = (\pi/a)(1,0,0)$, and then decreases to zero at the point X where $\mathbf{k} = (2\pi/a)(1,0,0)$ (the point group at X is D_{4h} and includes the inversion operation). Along the $[100][110]$ or Σ direction, the mixing is greatest at the point $\mathbf{k} = \pi/a(1,1,0)$. Because of the transformation properties listed in Table I, the $\text{Ag}^+ (4d)$ function located at the origin and the $\text{Cl}^- (3p)$ [or $\text{Br}^- (4p)$] function located at $\frac{1}{2}a(1,0,0)$ both have even parity at the point L . Consequently, this point is one of greatest p - d mixing along the $[111]$ direction.

For both AgCl and AgBr, the point at which the valence band maximum lies is difficult to determine. In either crystal both the uppermost Σ_4 and L_3 points have very nearly the same energy. For AgCl the Σ_4 eigenvalue is 0.001 Ry higher than that of L_3 ; in AgBr the L_3 state is 0.0177 Ry higher than that of Σ_4 . Thus the APW calculations do not clearly resolve the location of the valence-band maximum in either crystal.

⁹ J. Zak, J. Math. Phys. 3, 1278 (1962).

The APW valence bands for AgCl and AgBr are quite similar to those recently calculated by Bassani, Knox, and Fowler¹⁰ (henceforth abbreviated BKF) who used the tight-binding method. Although the techniques of calculation are quite different in the two methods, the only important differences in the results are that their Δ_1 and Δ_5 states for the highest valence bands in the [100] direction rise higher than those found by the APW method.

The most glaring discrepancy in the APW calculation is in the comparison of the calculated value of the indirect band gap with experiment. For both crystals the calculated indirect band gap is approximately 0.5 eV larger than the observed value.^{11,12} In the remainder of this paper we will consider possible corrections to the APW bands and show that the final calculations are consistent with experiment.

IV. ESTIMATES OF CORRECTION TERMS TO THE APW CALCULATION—INTRODUCTION

There are a number of possible causes for the discrepancy of 0.5 eV in the APW value of the indirect band gap. Some of these are: the lack of self-consistency in the calculation, errors in the ionic potentials employed, the effects of a varying potential outside the APW spheres, the effect of the nonspherical portion of the cubic field inside APW spheres, spin-orbit coupling, and other relativistic effects such as the Darwin and mass-velocity corrections.

In the absence of a self-consistent calculation it is very difficult to estimate how closely the present calculation approaches self-consistency. It is the opinion of the author that since the Herman-Skillman ionic potentials employed were self-consistent, and since the crystalline potential has been adjusted to fit the bands at Γ , that the APW calculation is not far from self-consistency.

Even though the Herman-Skillman potentials are self-consistent, the one-electron energies are higher than those determined by Hartree-Fock calculations because of the $\rho^{1/3}$ approximation. The $\text{Cl}^-(3p)$ eigenvalue is about 0.106 Ry higher, the $\text{Br}^-(4p)$ eigenvalue is 0.092 Ry higher, and the $\text{Ag}^+(4d)$ eigenvalue is 0.122 Ry higher. Since the bands were fit at Γ_{15} , only the variation of the difference between the Herman-Skillman and Hartree-Fock eigenvalues for the halogen and silver ions could affect the shapes of the energy bands (to first order). Because of the p - d mixing away from Γ , the uppermost Σ_4 and L_3 valence band states would be shifted downward relative to Γ_{15} by at most 0.01 Ry. This correction not only is small compared to the discrepancy in the indirect gap, but has the wrong sign (i.e., it would tend to increase the error).

¹⁰ F. Bassani, R. S. Knox, and W. B. Fowler, Phys. Rev. **137**, A1217, (1965).

¹¹ F. C. Brown, J. Phys. Chem. **66**, 2368 (1962).

¹² Y. Okamoto, Nachr. Akad. Wiss. Göttingen II Math. Physik. Kl. **1956**, 275 (1956).

For KCl, DeCicco¹³ has studied the effect of a varying cubic field outside APW spheres and the nonspherical cubic field inside APW spheres. He concluded that even though these fields vary substantially in the regions of interest, their net effect on the energy bands is quite small—usually of the order of a few thousandths of a rydberg for valence bands and rarely more than a hundredth of a rydberg for conduction bands. An estimate by first-order perturbation theory indicates that these effects are of the same order of magnitude in AgCl and AgBr. Since these corrections are roughly a factor of five or ten times smaller than the discrepancy we are trying to resolve, we may conclude that the effects of the cubic field not taken into account by the APW method are negligible.

The Herman-Skillman parameters which characterize the spin-orbit and mass-velocity effects for $\text{Cl}^-(3p)$, $\text{Br}^-(4p)$, and $\text{Ag}^+(4d)$ electrons are of the order of a few tenths of an electron volt. As we shall show in Secs. V and VI the spin-orbit splitting will not resolve the discrepancy of 0.5 eV, but the mass-velocity correction by itself can account for this error.

V. SPIN-ORBIT INTERACTION

As we shall show in this section, the spin-orbit interaction cannot account for the discrepancy in the size of the indirect band gap. However, since spin-orbit effects are of intrinsic interest, the details of the calculation will be discussed for three valence band states: Γ_{15} , and the Σ_4 and L_3 states at the valence band maximum along the [110] and [111] directions, respectively.

The APW wave functions at each of these three points in the Brillouin Zone were multiplied by the usual two-component spinors and the matrix elements for the spin-orbit operator were calculated. Because of the form of the APW potential energy, there are no contributions to the matrix elements from the region between spheres [$V(\mathbf{r}) = \text{constant}$ in this region]. Thus the spin-orbit matrix elements are a sum of terms arising from the regions inside the halogen and silver spheres. There are no overlap terms to be considered because of the form of the APW wave functions.

The spin-orbit interaction splits the Γ_{15} state into two levels: a fourfold-degenerate Γ_8^- state with energy $+\lambda$, and a doubly-degenerate Γ_6^- state with energy -2λ . For the Γ_{15} state, the amount of charge within the silver sphere is very small and to a good approximation one finds that

$$\lambda = \frac{\alpha^2}{4} \int_0^{R_h} \frac{1}{r} \frac{dV_h(r)}{dr} \rho_h(r) dr \quad \text{Ry.}$$

Here α is the fine-structure constant (equal to 1/137), $\rho_h(r)$ is the spherically-averaged radial charge density within the halogen sphere, $V_h(r)$ is the halogen free-ion

¹³ P. DeCicco, MIT Solid-State and Molecular Theory Group, Quarterly Progress Report No. 54, October 1964 (unpublished).

potential energy, and R_h is the radius of the halogen sphere. If $\rho_h(r)$ were exactly equal to the free-ion charge density and R_h were replaced by infinity, λ would equal one half the free-ion spin-orbit parameter. However, since the halogen wave function is slightly compressed in the crystal, λ turns out to be about 10% higher than its free-ion value. For AgCl, $\lambda=0.0033$ Ry and the $\Gamma_8^- - \Gamma_6^-$ splitting (equal to 3λ) is 0.0099 Ry or 0.13 eV; for AgBr $\lambda=0.0143$ Ry and the splitting is 0.0429 Ry or 0.58 eV.

When spin is included, all bands in the $[110]$ or Σ direction are doubly degenerate and have symmetry Σ_5 . At the valence band maximum in this direction the spin-orbit perturbation is zero to first order; the energy is shifted in second order by an amount $\lambda^2(\Delta E)^{-1}$ where λ is of the order of the appropriate spin-orbit parameters and ΔE is the difference in energy of a neighboring band. For AgCl and AgBr this shift is roughly a few thousandths of a rydberg and may be safely neglected.

The L_3 state at the valence band maximum in the $[111]$ direction is split by the spin-orbit interaction into two levels: a doubly-degenerate L_6^+ state and L_4^+ and L_5^+ states which are degenerate with each other because of time reversal symmetry. The energy levels are given by $\pm\epsilon$ (L_4^+ and L_5^+ have energy $+\epsilon$, L_6^+ has energy $-\epsilon$) where

$$\epsilon = \begin{cases} \lambda_{3p}^c - K\lambda_{4d}^s & \text{for AgCl,} \\ \lambda_{4p}^b - K\lambda_{4d}^s & \text{for AgBr.} \end{cases}$$

Here K is a parameter which is a measure of the distortion of the Ag^+ free-ion wave function by the cubic field. For zero cubic field, K would equal unity; for AgCl, $K=0.67$; for AgBr, $K=0.83$ (AgBr has a larger lattice constant than AgCl and hence a smaller cubic field strength). After approximating λ_{ni} by $(q_i)^{\frac{1}{2}} \zeta_{ni}$ and inserting the numerical values of the q 's, ζ_{ni} 's and K 's, one obtains $\epsilon = -0.0032$ Ry for AgCl and $\epsilon = +0.0029$ Ry for AgBr. Thus, first-order perturbation theory gives a small splitting at L_3 , and indicates that in AgBr L_4^+ and L_5^+ lie above L_6^+ ; in AgCl the L_6^+ state is highest. Since the magnitude and sign of ϵ depend on the difference of two almost identical numbers, either of which may be error by ten percent, these results are far from being precise. However, we may conclude that the spin-orbit splitting at L_3 should be less than 0.007 Ry or 0.1 eV.

VI. MASS-VELOCITY PERTURBATION

The mass-velocity perturbation may be approximated by a spherically-symmetric operator about each site in the crystal. Since the electron's speed is largest in the neighborhood of the nucleus, we ignore the mass-velocity effect for the plane waves between APW spheres, and restrict ourselves to calculating the correction to a given energy level by considering only the portion of the wave function within spheres.

Using first-order perturbation theory, an APW level

is shifted by

$$\Delta E(\mathbf{k}) = \sum_i [q_{ih}(\mathbf{k})\nu_{ih} + q_{is}(\mathbf{k})\nu_{is}],$$

where the q_i 's are the amounts of charge within the halogen and silver spheres associated with the APW state, and the ν_i 's are the ionic mass-velocity parameters.

We must now determine the mass-velocity parameters. For a first estimate we can use the free-ion parameters since the radial wave functions within APW spheres for the free ions and the crystal are substantially the same, especially near the nucleus where the mass-velocity effect is largest.

For the free ions, Herman and Skillman calculated the mass-velocity shift by first-order perturbation theory, averaging the mass-velocity operator $V' = -\alpha^2(E-V)^2$ over the free-ion wave function. However, a more accurate calculation has been performed by Waber¹⁴ who solved the Dirac equation for the energies of the two possible j values of a given electron. By taking the appropriate weighted average of Waber's two eigenvalues one obtains the energy for an electron with all relativistic effects included with the exception of spin-orbit coupling.

In Table II, we compare the Herman-Skillman and Waber calculations for $\text{Cl}^-(3p)$, $\text{Br}^-(4p)$, and $\text{Ag}^+(4d)$ ionic eigenvalues. Waber's eigenvalues are higher than those of Herman-Skillman for every case shown. This may be explained by the fact that the mass-velocity operator in reality produces two effects for a valence electron:

1. It lowers the eigenvalue because the mass-velocity operator is always negative.
2. It raises the eigenvalue because the core electrons are drawn closer to the nucleus, producing a stronger inner shielding of the nucleus.

The Herman-Skillman calculation ignores the second effect which, as Waber's calculation indicates, is actually greater in magnitude than the first.

It is interesting to note that Waber's eigenvalues are very close to the Herman-Skillman nonrelativistic energies. Therefore, in our perturbation calculation, we may approximate the mass-velocity parameters by the difference of the Waber and Herman-Skillman (non-relativistic) levels given in column four of Table II. After using these mass-velocity parameters and the appropriate q_i 's, one obtains the following shifts in energy for the uppermost valence bands at Γ_{15} , Σ_4 , and L_3 (in rydbergs):

	Γ_{15}	Σ_4	L_3	
	+0.0002	+0.0389	+0.0399	AgCl
	+0.0009	+0.0343	+0.0269	AgBr.

Thus the mass-velocity perturbation raises the Σ_4 and L_3 states relative to the Γ_{15} state by 0.37 to 0.55 eV, a large correction that virtually eliminates any discrepancy in the final value for the indirect band gap.

¹⁴ J. Waber (private communication).

TABLE II. Comparison of Herman-Skillman^a and Waber free-ion eigenvalues.

	<i>H-S</i> (nonrelativistic)	<i>H-S</i> (including mass-velocity)	Waber (relativistic)	Waber minus <i>H-S</i> (nonrelativistic)
Cl ⁻ (3 <i>p</i>)	-0.19094587	-0.19794587	-0.1906440	+0.00030187
Br ⁻ (4 <i>p</i>)	-0.18183391	-0.21283391	-0.1807204	+0.00104187
Ag ⁺ (4 <i>d</i>)	-1.5682048	-1.6152048	-1.5082592	+0.0599456

^a The Herman-Skillman mass-velocity energy was found by interpolation from their tables which list only the energies for atoms with even *Z*.

VII. FINAL RESULTS AND COMPARISON WITH EXPERIMENT

We shall present only a few remarks on the over-all band structures of AgCl and AgBr since BKF have given a detailed analysis of the experimental data and its relationship to the energy bands.

The value of the indirect band gap found by the APW method is about 0.5 eV too small for both AgCl and AgBr. After a preliminary survey of several possible correction terms omitted in the APW calculation, it was shown that the mass-velocity correction by itself could account for the discrepancy. In Table III we compare the calculated values for the direct and indirect band gaps. By examining Table III one can see that the mass-velocity correction is needed in order that the calculated value for the indirect band gap be in reasonable agreement with experiment.

The energies for the Σ_4 and L_3 points at the valence-band maximum in the [110] and [111] directions, respectively are practically identical in both crystals after the mass-velocity correction has been included. For AgCl the energies are equal to within 0.01 eV, for AgBr the L_3 state is about 0.1 eV higher. Thus the location of the valence-band maximum cannot be clearly determined in either crystal; BKF indicate that both possibilities are consistent with experiment.

At Γ_{15} the spherically-averaged radial charge density inside the halogen sphere was compared with that of the free ion (found from Herman-Skillman's program). For both AgCl and AgBr, the crystalline charge density was slightly larger near the nucleus than in the free ion, accounting for the larger spin-orbit splittings. For

AgBr the calculated splitting is about 0.58 eV and is in agreement with experiment; for AgCl the calculated splitting is 0.13 eV and more than twice the observed value. A plausible explanation for the smaller splitting in AgCl may be given in terms of many-body effects.¹⁵

At L_3 the spin-orbit contributions from the halogen and silver ions have opposite sign. The theoretical upper limit to the splitting is 0.1 eV and is in agreement with the observed exciton splitting in both crystals.

The details of the conduction bands hypothesized by BKF do not agree with those calculated by the APW method, the chief difference occurring for the symmetry labels at L . In the absence of a calculation BKF tentatively assigned the lowest conduction band to have $L_{2'}$ symmetry (L_1 in our convention) and the second lowest conduction band to have L_1 symmetry ($L_{2'}$ in our convention). Strictly speaking, because of parity, electric dipole transitions can occur only between primed and unprimed states at L . However, since one may consider $L_1 \rightarrow L_3$ transitions (which actually take place near L) in the sense described by Phillips,¹⁵ the parity of the states at L is not of the utmost importance.

VIII. CONCLUSIONS

The band structure for both AgCl and AgBr appear to be in quite reasonable agreement with experimental facts. The success of this calculation not only illustrates the validity of the energy band method but shows that many of the details of the crystalline potential not explicitly taken into account by the APW method are negligible. Furthermore, the importance of relativistic corrections and their effect on some of the important features of the over-all band structure has been demonstrated.

ACKNOWLEDGMENT

The author wishes to thank Professor John Wood under whose supervision this work was performed. He also would like to thank the members of the Solid State and Molecular Theory Group of the Massachusetts Institute of Technology for their discussions and assistance, especially Dr. A. C. Switendick who supplied virtually all of the necessary computer programs. Finally, the author thanks Professor J. C. Slater for his many comments and suggestions regarding the manuscript.

TABLE III. Comparison of calculated and experimental^a values for band gaps.

	Direct gap (at $k=0$) E_g	Indirect gap, E_{ig} (experimental)	E_{ig} (Calculated- APW)	E_{ig} (Calculated APW and mass- velocity)
AgCl	5.13 eV	3.25 eV	3.84 eV	3.28 eV
AgBr	4.29 eV	2.68 eV	3.24 eV	2.89 eV

^a The experimental values quoted for the band gaps are the values of the absorption edges and have not been corrected for the exciton binding energy which is of the order of a few tenths of an electron volt (based on a hydrogenic model). If the exciton binding energy were constant for all k values, one could (because of the fitting procedure employed) correct all the experimental and calculated values listed by simply adding this constant. However, since the valence and conduction bands have considerable width, the exciton bands will exhibit k dependence. In the absence of a detailed knowledge of the exciton bands, these corrections were not included in the present calculation.

¹⁵ J. C. Phillips, Phys. Rev. **136**, A1705, A1714, A1721 (1964).